Pharmacophore

Original Research Paper

2D & 3D QSAR STUDIES OF BIARYL ANALOGUES OF PA-824 HAVING VARIOUS ETHER LINKERS: AN APPROACH TO DESIGN ANTITUBERCULAR AGENTS

Sawarkar Vaibhav M, **Dudhe Prashik B***, Nagras Madhuri A, Bhosle Pallavi V,

Jadhav Supriya B and Meshram Rutuja S

Department of Pharmaceutical Chemistry, S. T. E. S's, Sinhgad College of Pharmacy,

S. No. 44/1, Vadgaon (Bk), off. Sinhgad Road, Pune-411041, India

ABSTRACT

New analogues of PA-824 having alternative side chain ether linkers of varying size & flexibility shows 8-fold better activity than parent drug i.e. PA-824 as Mycobacterium tuberculosis (M.tb.) inhibitors. Recent work suggests that bicyclic nitroimidazole-based prodrugs PA-824 as intracellular nitric oxide (NO) releaser is key to their activity against non replicating persistent M.tb. 2D & 3D QSAR studies were performed on a set of 72 Biaryl analogues of PA-824 having various ether linkers using V-Life Molecular Design Suite (MDS 3.5) QSAR plus module. The best model were generated using Multiple linear regression (MLR) analysis ($r^2 = 0.8416$, $q^2 = 0.7853$, F test = 47.8273, pred_$r^2 = 0.8481$, pred_r^2se = 0.2880) and Principle Component Regression (PCR) ($r^2 = 0.7781$, $q^2 = 0.7274$, F test = 42.517, pred_$r^2 = 0.8405$, pred_r^2se = 0.2951) for 2D and 3D QSAR respectively. For each set of descriptors, the best multi-linear QSAR equations were obtained by the stepwise variable selection method using leave-one-out cross-validation as selection criterion. Alignment independent descriptors were the most important descriptors in predicting antitubercular inhibitory activity. New Chemical Entities (NCEs) were designed using results of QSAR studies.

Keywords: Mycobacterium tuberculosis inhibitors, PA-824, V-life, QSAR, CombiLib.

INTRODUCTION

Mycobacterium tuberculosis (M.tb.) is the causative agent of tuberculosis (TB). It has a strong ability to persist in the human host.[1] The currently prevailing scenarios of drug-resistant tuberculosis (TB) are particularly alarming, and pose a significant threat to the control of the disease globally.[2] Host cells can impose immunity through the bacteriostasis effects of endogenous reactive nitrogen species (RNS), reactive oxygen species (ROS) and nutrient depravation, all of which can drive M.tb. into its non replicating state, a state also reached in hypoxia.[3,4] As most frontline drugs are used to kill replicating Mtb, the non replicating state of Mtb is persistent.

Promising new candidate drugs are the bicyclic nitroimidazole PA-824, which are currently in human clinical trials.[5,6] Nitroimidazole-based prodrugs PA-824 were initially characterized as mycolic acid synthesis inhibitors demonstrating high in vitro potencies against both susceptible and resistant M.tb. and excellent efficacies in animal models, either alone or in combination with other agent.[7] Recent work suggests that intracellular nitric oxide (NO) release is key to their activity against non replicating persistent M.tb.[8,9] The bicyclic nitroimidazole PA-824 is a pro-drug with a very complex mechanism of action active against both replicating and hypoxic, non-replicating Mycobacterium tuberculosis.

Microarray analysis of the mode of action of PA-824 showed a puzzling mixed effect both on genes responsive to both cell wall inhibition (like isoniazid) and respiratory poisoning (like cyanide) It has been shown that PA-824 acts directly as an NO donor. Based on metabolite profiling of PA-824 it has been recently shown that these bicyclic nitroimidazoles act as (NO) donors, and that NO release from various PA-824 derivatives correlated well with the anaerobic killing of M.tb. This NO-releasing effect of PA-824 is sufficient to kill aerobically replicating cells. Within mycobacterial cells NO reacts with cytochromes/cytochrome oxidase to interfere with the metabolism, electron flow and ATP homeostasis under hypoxic non-replicating conditions. This anaerobic activity by PA-824 is called respiratory poisoning.

The effect of PA-824 on the respiratory complex under hypoxic non-replicating conditions was also manifested in a rapid drop in intracellular ATP levels, again similar to that observed by cyanide treatment. Thus, transcriptional profiling provided valuable clues to elucidating the molecular mechanism of mycobacterial killing. Treatment with PA-824 disrupts the formation of mycolic acids, major constituents of the cell envelope of M.tb. However, this effect seemed unlikely to be responsible for cell killing under nonreplicating conditions, because the bacilli do not restructure mycolic acids under anaerobic conditions. So taking all these factors in consideration different analogues of PA-824 having various ether linkages could be developed as anti TB drugs.[9]

We selected 72 molecules belonging to bicyclic nitroimidazole derivative as M.tb. inhibitor from the published articles of Andrew M. Thompson et al. These reported series of bicyclic nitroimidazole derivatives shows wide variation in structures and activity.[8-10] Uptil now there is no 2D and 3D QSAR has been performed on bicyclic nitroimidazole derivatives. In this work we have performed 2D and 3D QSAR analysis on M.tb. inhibitor with anti-tuberculosis activity by using V-Life MDS software. Regression methods like multiple regression, principle component

regression were used to build QSAR models in the form of mathematical equation. These equations explain the importance of every independent variable (descriptors) against dependent variable (usually activity).
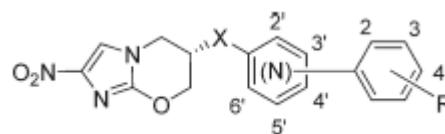
General structure of bicyclic nitroimidazole [Bicyclic nitroimidazole derivatives as Antituberuular agents[9] (Table 1)]

COMPUTATIONAL METHODS
MATERIAL & METHOD
Chemical Data

The set of 72 molecules were belonging to Biaryl analogues of PA-824 having various ether linkers as Mycobacterium tuberculosis inhibitor drugs. The reported series of Biaryl analogues of PA-824 showed wide variations in their structures, potency profiles and thus used for the study The negative logarithm of the measured IC50 (μM) against M.tb**.** As pIC50 [pIC50 = $-$log (IC50 X 10^{-6})] was used as dependent variable, thus correlating the data linear to the free energy change. Since some compounds exhibited insignificant/no inhibition, such compounds were excluded from the present study. The whole dataset was randomly divided into a training set of 51 compounds and a test set of 21 compounds.[9] The training set was used to construct the 2D & 3D-QSAR models and the test set was used for the models validation.

Data set/ Molecular Modeling Study

All QSAR studies were performed in V-Life MDS software Version 3.5. Two dimensional descriptors were calculated using V-Life MDS software[11] which included various physico-chemical, structural, topological, electro-topological, Baumann alignment independent topological descriptors[12] and Merck Molecular Force Field (MMFF) atom type count descriptors. Molecular modeling and MLR studies were performed on DELL computer having genuine Intel Pentium Dual Core Processor and Windows XP operating system using the software Molecular Design Suite (MDS). The relationship between biological activities and various

descriptors (Physiochemical and alignment-independent) were established by sequential multiple regression analysis (MLR) using MDS 3.5, in order to obtain QSAR models. All the compounds were drawn in ChemBioDraw Ultra (version 12.0.2) using fragment database and then subjected to energy minimization using batch energy minimization method. All the structures were minimized using the standard MMFF with the distance dependant dielectric function and an energy gradient of 0.001kcal/mol A.

Selection of Training and Test Set
The set of 72 molecules were belonging to Biaryl analogues of PA-824 having various ether linkers as M.tb. inhibitor drugs. Optimal training and test sets for QSAR were generated using sphere exclusion algorithm.

2D QSAR
2D QSAR study was done by Multiple Linear Regression Method (MLR) using forward-backward stepwise variable selection method, The MLR analysis was used to correlate biological activities with physicochemical properties and in turn chemical composition of the selected series of compounds. MLR is the standard method for multivariate data analysis. For getting reliable results, parameters were set such that the regression equation should generate number of independent variables (descriptors) five times less than that of points (molecules). The regression equation takes the form as mentioned in
Eq. 1: $Y = b_1 * x_1 + b_2 * x_2 - b_3 * x_3 + c$ ….. (1)
Where, Y is the dependent variable (Biological activity, PIC_{50}), the 'b1 to b3' are regression coefficients (contribution of respective descriptors that is, x1 to x3), 'x1 to x3' are independent variables (Descriptors), and 'c' is a regression constant or intercept.

3D QSAR
3D QSAR modeling was performed using stepwise forward-backward PCR method that adopts a principle for generating relationship between molecular field and apoptosis- inducing activity. The stepwise forward-backward PCR model were generated using training set of same as 2D QSAR i.e. 51training set compound and 3D

QSAR models were validated using a test set of 21compounds. The steric (S) and electrostatic (E) descriptors specify the regions, where variation in the structural features of different compounds in training set leads to increases or decreases in activities. The number accompanied by descriptors represents its position in 3D PCR grid. The stepwise forward- backward variable selection method resulted in several statistically significant models. The model selection criterion is the value of r^2, q^2, internal predictive ability of model, and that of $pred\_r^2$, ability of the model to predict activity of external test set.

Model Validation
This is done to test the internal stability and predictive ability of the QSAR models. Developed QSAR models were validated by the following procedure:

Internal Validation
Internal validation was carried out using leave-one-out (q2, LOO) method. The cross-validated r2 (*q*2) value was calculated using eq. 1, where *yi* and *yˆi* are the actual and predicted activities of the *i*th molecule, respectively For calculating q2, each molecule in the training set was eliminated once and the activity of the eliminated molecule was predicted by using the model developed by the remaining molecules, and *y* mean is the average activity of all molecules in the training set.

$$q^2 = 1 - \frac{\sum(y_1 - \hat{y}_i)}{\sum(y_i - y_{mean})^2}$$ ……. (2)

External Validation
For external validation, the activity of each molecule in the test set was predicted using the model developed by the training set. The pred_r2 value is calculated as follows.

$$pred\_r^2 = 1 - \frac{\sum(y_1 - \hat{y}_i)^2}{\sum(y_i - y_{mean})^2}$$ …… (3)

Where *yi* and *ˆyi* are the actual and predicted activity of the *i*th molecule in the training set, respectively, and *y*mean is the average activity of all molecules in the training set. Both summations are over all molecules in the test set. Thus, the

pred_r2 value is indicative of the predictive power of the current model for external test set.

DESIGN OF NCES

The findings of 2D and 3D QSAR studies provide the overall substitution pattern (electrostatic, steric and hydrophobic pattern) required around the pharmacophore. Substitution pattern around the pharmacophore showed in (Figure 5) was used for the design of NCEs using CombiLib tool of V-Life MDS software. The parameters used as Lipinski's filters are[13,14]

- Number of hydrogen bond acceptor (A) (<10).
- Number of hydrogen bond donor (D) (<5).
- Number of rotatable bond (R) (<10).
- Xlog P (X) (<5).
- Molecular weight (W) (<500 g/ mol).
- Polar surface area (S) is (<140 Å).

Designed compounds should pass through Lipinski's screen (ADRXWS) to ensure drug like pharmacokinetic profile of the designed compounds in order to improve their bioavailability.

RESULT & DISCUSSION

QSAR was the study of the quantitative structural activity relationship between the experimental activity of a set of compounds and their physicochemical properties using statistical methods. The molecular structures of the compounds in series were sketched by using V-Life MDS module of V-Life science molecular modeling software. The molecules then transferred to three-dimensional structures (3D). The basis of energy minimization is that the drug binds to effectors/receptor in the most stable form i.e. minimum energy state form.

2D QSAR

Two dimensional descriptors were calculated and the relationship between biological activities and various descriptors (Physiochemical and alignment independent) were established by Multiple Linear Regression Analysis (MLR) in order to obtain QSAR models. The V-Life MDS 3.5 program was employed for the calculation of different quantum chemical descriptors including heat of formation, dipole moment, local charges and different topological descriptors. Further chemical parameters including molecular polarizability (MP), Hydration energy (HE), Hydrogen acceptor count (HAC), Hydrophobicity (log P), Molecular surface area (SA), molar volume (V) were also calculated. By optimizing the molecules the best 2D QSAR model was generated along with the variation of the descriptors in these models. The fitness plot (Fig. 2) of observed activity on x-axis versus predicted activity on y-axis for 2D QSAR model was also generated for evaluating the dependence of the biological activity on various different types of the descriptors. The frequency of particular descriptor in the population of equations indicates the relevant contributions of that descriptor in the activity. According to the values of the r^2 and q^2 the best regression equation selected was given below. The statistical result of 2D QSAR model along with the contribution of the descriptors are tabulated in table 2.

2D QSAR study by Multiple Linear Regression method using forward-backward stepwise variable selection method, the final QSAR equation was developed having 5 variables as follows:

PIC50 = 0.5337(T_N_O_6)-0.1704(T_2_N_7)-0.5104(T_N_N_7)-0.5074(T_N_O_3) 0.1063(T_C_O_4)……. (4)

T_N_O_6

This is Alignment Independent (AI) descriptor signifies the count of number of Nitrogen atoms (single, double or triple bonded) separated from any oxygen atom (single, double or triple bonded) by 6 bond distance in a molecule. This descriptor showed positive contribution toward inhibitory activity in selected QSAR equation and its contribution is approx 31.07% (Figure 2). Positive contribution of this descriptor was clearly signifying that the distance between Nitrogen and Oxygen atoms should be more than 6.

T_N_O_3

This is Alignment Independent (AI) descriptor signifies the count of number of Nitrogen atoms (single, double or triple bonded) separated from any oxygen atom (single, double or triple bonded)

by 3 bond distance in a molecule. This descriptor showed positive contribution toward inhibitory activity in selected QSAR equation and its contribution is approx -21.02% (Figure 2). Negative contribution of this descriptor was clearly signifying that the distance between Nitrogen and Oxygen atoms should be less than 3.

T_2_N_7

This is also Alignment Independent (AI) descriptor signifies the count of number of double bonded atom (i.e. any double bonded atom, T_2) separated from Nitrogen atom by 7 bonds. This is negatively contributing descriptor in selected 2D QSAR equation and its contribution is approx -28.64% (Figure 2).

T_N_N_7

This is Alignment Independent (AI) descriptor signifies the count of number of any atoms (single, double or triple bonded) separated from any other Nitrogen atom (single, double or triple bonded) by 3 bonds in a molecule. This is negatively contributing descriptor in selected 2D QSAR equation and its contribution is approx -12.80% (Figure 2).

T_C_O_4

This is the count of number of Carbon atoms (single double or triple bonded) Separated from any Oxygen atom (single or double bonded) by 4 bond distance in a molecule. This is negatively contributing descriptor in selected 2D QSAR equation and its contribution is approx -6.47% (Figure 2). The observed activity vs. predicted activity is shown in (Figure 1).
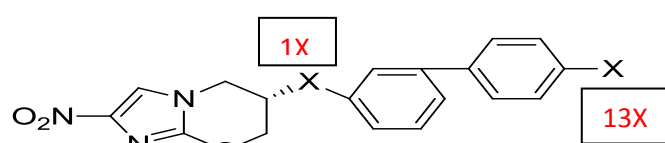
3D QSAR

In 3D QSAR studies, 3D data points generated around bicyclic nitroimidazole pharmacophore were used to optimize the electrostatic, hydrophobicity & steric requirements of the bicyclic nitroimidazole nucleus for M.tb. inhibitory activity (Figure 4). The range of

property values in the generated data points helped for the design of NCEs. These ranges were based on the variation of the field values at the chosen points using the most active molecule and its nearest neighbour set. The points generated in PCR 3D QSAR model was H_1255 (3.0380), E_708 (-0.1076), S_983 (0.0227), S_1739 (3.2274) i.e., hydrophobic, electrostatic & steric interaction field at lattice points 1255, 708, 983 and 1739, respectively. Results obtained and point generated around the pharmacophore using the 3D QSAR studies was used for correlation chemical nature of substituent around the pharmacophore with their observed activity (Figure 3 & 4). The Results of 2D & 3D QSAR is shown in table 2.

DESIGN OF NEW CHEMICAL ENTITIES (NCEs) CONTAINING BICYCLIC NITROMIDAZOLE PHARMACOPHORE

The findings of 2D and 3D QSAR studies provided the overall substitution pattern (electrostatic, steric and hydrophobic pattern) required around the bicyclic nitroimidazole pharmacophore (Figure5). Descriptors generated in 2D QSAR equation signified the importance of bicyclic nitroimidazole nucleus for inhibitory activity of compounds. Similarly electrostatic, hydrophobic & steric points generated around common template or pharmacophore in 3D QSAR suggested substitution of electronegative hydrophobic group at ether linking position, and steric substitution at side chain position around bicyclic nitrimidazole ring. This information had helped a lot in optimizing bicyclic nitroimidazole pharmacophore and designing of NCEs as M.tb.inhibitors.

Structure of designed NCEs along with predicted activity obtained by MLR equation generated by 2D QSAR (Table 3)
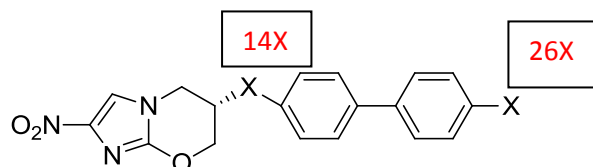
Structure of designed NCEs along with predicted activity obtained by MLR equation generated by 2D QSAR (Table 4)
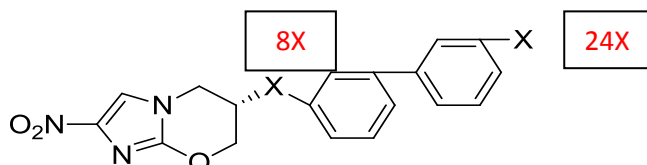
Structure of designed NCEs along with predicted activity obtained by MLR equation generated by 2D QSAR (Table 5)

CONCLUSION

From the detail study of 2D QSAR it was observed that the descriptors which are highly correlated with the biological activity of bicyclic nitrimidazole (biaryl analogues of PA-824) series are (T_N_O_6), (T_2_N_7), (T_N_N_7), (T_N_O_3), and (T_C_O_4). T_N_O_6 showed positive contribution to the biological activity while (T_2_N_7), (T_N_N_7), (T_N_O_3), (T_C_O_4) showed negative contribution to the biological activity. It can be concluded that M.tb. inhibitory activity of Biaryl analogues of PA-824 is strongly influenced by the alignment independent descriptor. Analysis of 3D counter plot generated in 3D QSAR study provides details on the fine relationship linking structure and activity and offers clues for structural modifications that can improve the activity. These trends should prove to be an essential guide for the future work. The descriptors showed by QSAR study can be used further for study and design of new compounds. Consequently this study may prove to be helpful in development and optimization of existing antituberculosis activity of this class of compounds. The designed compounds may found to be good pharmacophore for the further development of M.tb. inhibitors.

ACKNOWLEDGEMENT

Table 1: Bicyclic nitroimidazole derivatives as Antitubercular agents

Compd.	Substituents				IC$_{50}$ (MABA)	PIC$_{50}$		
	link	Aza	X	R		Observed	Predicted	
							2D	3D
1.	4′		O	4-OCF$_3$	0.090	10.0457	9.5860	9.6254
2.	4′		O	4-F	0.31	9.5086	9.6923	9.3911
3.	4′		O	4-CF$_3$	0.39	9.4089	9.6923	9.6423
4.	4′		O	3-aza, 4-CF$_3$	0.51	9.2924	9.5219	9.5084
5.	3′	2′	O	4-F	3.2	8.4948	9.1012	8.9680
6.	3′	2′	O	4-CF$_3$	0.55	9.2596	9.1012	9.1283
7. T	3′	2′	O	3-aza, 4-CF$_3$	5.7	8.2441	8.9308	9.0419
8.	3′	2′	O	4-OCF$_2$H	0.52	9.2839	8.9949	9.0742
9.	3′	4′	O	4-OCF$_3$	0.30	9.5228	9.3093	9.2069
10. T	3′	4′	O	4-F	0.67	9.1739	9.4156	9.0345
11.	3′	4′	O	4-CF$_3$	0.65	9.1870	9.4156	9.1974

12.	3′	6′	O	4-OCF₃	5.1	8.2924	8.6542	8.4626
13. T	3′	6′	O	4-F	5.2	8.2639	8.7604	8.5796
14.	3′	6′	O	4-CF₃	0.88	9.0555	8.7604	8.5236
15.	3′	6′	O	3-aza, 4-CF₃	3.0	8.5226	8.5900	8.7202
16. T	3′	4′,6′	O	4-OCF₃	2.1	8.6777	8.6542	8.6536
17. T	3′	4′,6′	O	4-CF₃	0.80	9.0969	8.7604	8.9704
18. T	3′	4′,6′	O	3-aza, 4-CF₃	3.0	8.5228	8.5900	8.7834
19.	4′	2′	O	4-OCF₃	0.39	9.4089	9.1012	9.4419
20. T	4′	2′	O	4-F	0.37	9.4317	9.2075	9.2095
21. T	4′	3′	O	4-F	0.50	9.3010	9.1819	9.2565
22.	4′	3′	O	4-CF₃	0.78	9.1079	9.1819	9.5032
23.	4′	3′	O	3-aza, 4-CF₃	0.45	9.3467	9.0115	9.3770
24.	4′	2′,6′	O	4-F	1.6	8.7958	8.7227	9.0540
25.	4′		OCH(Me)	4-OCF₃	0.19	9.7212	9.8205	9.6577
26.	4′		OCH(Me)	4-F	0.22	9.6575	9.9268	9.5679
27.	4′		OCH(Me)	4-CF₃	0.18	9.7447	9.9268	9.8406
28. T	4′		OCH(Me)	3-aza, 4-CF₃	0.39	9.4089	9.7564	9.6845
29.	4′		O(CH₂)₃	4-OCF₃	0.15	9.8239	10.0971	10.3115
30.	4′		O(CH₂)₃	4-F	0.045	10.3467	10.2034	10.2565
31.	4′		O(CH₂)₃	4-CF₃	0.043	10.3665	10.2034	10.4633
32.	4′		O(CH₂)₃	3-aza, 4-CF₃	0.07	10.1549	10.0330	10.2004
33.	4′		O(CH₂)₂O	2-aza, 4-CF₃	0.055	10.2596	10.2034	10.3327
34.	4′		O(CH₂)₂O	4-OCF₃	0.055	10.2596	10.4183	10.3261
35.	4′		O(CH₂)₂O	4-F	0.04	10.3979	10.5246	10.1433
36.	4′		O(CH₂)₂O	4-CF₃	0.04	10.3979	10.5246	10.3607
37.	4′		O(CH₂)₂O	3-aza, 4-CF₃	0.025	10.6020	10.3542	10.2204
38.	4′	2′	O(CH₂)₂O	4-OCF₃	0.04	10.3979	10.2743	9.9291
39.	4′	2′	O(CH₂)₂O	4-F	0.02	10.6989	10.3805	10.6054
40.	4′	2′	O(CH₂)₂O	4-CF₃	0.02	10.6989	10.3805	9.9770
41.	4′	2′	O(CH₂)₂O	3-aza, 4-CF₃	0.22	9.6575	9.6998	9.7243
42.	4′	2′,6′	O(CH₂)₂O	4-OCF₃	0.13	9.8860	10.1302	9.8275
43.	4′	2′,6′	O(CH₂)₂O	4-F	0.13	9.8860	10.2365	10.0109
44. T	4′	2′,6′	O(CH₂)₂O	4-CF₃	0.12	9.9208	9.0453	9.9076
45.	4′	2′,6′	O(CH₂)₂O	3aza, 4-CF₃	0.63	9.2006	10.2365	9.6320
46.	4′		OCH₂CH=CH	4-OCF₃	0.063	10.2006	9.9268	10.2691
47.	4′		OCH₂CH=CH	4-F	0.09	10.0457	10.0330	9.8607
48. T	4′		OCH₂CH=CH	4-CF₃	0.045	10.3467	9.9268	10.2154
49.	4′		OCH₂CH=CH	4-OCF₂H	0.08	10.0969	10.0330	10.2129
50.	4′		OCH₂C≡C	4-OCF₃	0.16	9.7958	10.0971	10.5570
51.	4′		OCH₂C≡C	4-F	0.035	10.4559	10.2034	10.3610
52. T	4′		OCH₂C≡C	3-aza, 4-CF₃	0.15	9.8239	10.2034	10.0666
53. T	4′		OCH₂C≡C	4-OCF₂H	0.14	9.8538	10.0330	10.4408
54. T	4′		OCH₂C≡C	4-OCF₃	0.11	9.9586	10.0971	9.5610
55.	3′		OCH₂C≡C	4-F	0.04	10.3979	10.0971	10.3757
56.	3′		OCH₂C≡C	3-aza, 4-CF	0.12	9.9208	10.0330	10.0003
57.	3′		OCH₂C≡C	4-OCF₂H	0.09	10.0457	10.0971	10.0492
58.	3′	2′	OCH₂C≡C	4-OCF₃	0.025	10.6020	10.2365	10.4835
59. T	4′	2′	OCH₂C≡C	4-F	0.05	10.3010	10.2365	10.2900
60.	4′	2′	OCH₂C≡C	4-CF₃	0.02	10.6989	10.5668	10.4180
61.	4′	2′	OCH₂C≡C	3-aza, 4-CF₃	0.44	9.3565	9.9267	9.8345
62.	4′	2′	OCH₂C≡C	4-OCF₂H	0.025	10.6020	10.2034	10.3552
63. T	4′	3′	OCH₂C≡C	4-OCF₃	0.09	10.0457	10.3106	10.1983

64.	4′	3′	OCH₂C≡C	4-F	0.05	10.3010	10.0971	10.3159
65.	4′	3′	OCH₂C≡C	4-CF₃	0.07	10.1549	10.0971	10.2169
66. T	4′	3′	OCH₂C≡C	3-aza, 4-CF₃	0.12	9.9208	10.0330	9.8805
67.	4′	3′	OCH₂C≡C	4-OCF₂H	0.08	10.0969	10.0330	10.0764
68. T	4′		O(CH₂)₃C≡C	4-OCF₃	0.055	10.2596	9.9267	10.2233
69. T	4′		O(CH₂)₃C≡C	4-F	0.07	10.1549	10.2675	10.0764
70. T	4′		O(CH₂)₃C≡C	4-CF₃	0.085	10.0757	10.3738	10.2160
71.	4′		O(CH₂)₃C≡C	3-aza, 4-CF₃	0.11	9.9586	10.3738	9.7666
72. T	4′		O(CH₂)₃C≡C	4-OCF₂H	0.035	10.4559	10.2675	10.1212

*T- Test set

Table 2: Statistical parameters of 2D & 3D model generated by MLR & PCR method resp. for M.tb. inhibitory activity

Statistical Parameter	2D Result	3D
r^2	0.8416	0.7871
r^2 se	0.2545	0.2918
q^2	0.7853	0.7274
q^2 se	0.2963	0.3302
pred_r^2	0.8481	0.8405
pred_r^2se	0.2963	0.2951
F test	47.8273	42.5117
N	51	51
Contributing descriptors	T_N_O_6 (+) T_2_N_7 (-) T_N_N_7 (-) T_N_O_3 (-) T_C_O_4 (-)	H_1255 (+) S_983 (+) S_1739 (+) E_708 (-)

r^2 –quantity of determination, q^2- cross validation, N- no. of groups

Table 3: Structure of designed NCEs along with predicted activity obtained by MLR equation generated by 2D QSAR

Comp.	1X	13X	Screen result	Screen score	Predicted activity
1	cyclopropane	imidazole	ADRXWS	6	12.2283
2	cyclopropane	2-thiophene	ADRXWS	6	12.7143
3	cyclopropane	2-oxazolyl	ADRXWS	6	12.1583
4	cyclopropane	2-pyridyl	ADRXWS	6	12.8149
5	cyclobutane	imidazole	ADRXWS	6	12.5833
6	cyclobutane	2-imidazolyl	ADRXWS	6	12.0314
7	cyclopentane	2-pyrazinyl	ADRXWS	6	11.8718
8	cyclopentane	2-imidazolyl	ADRXWS	6	11.7613
9	carboxylate	imidazole	ADRXWS	6	11.0487
10	carboxylate	2-imidazolyl	ADRXWS	6	11.0518

11	carboxylate	3-isoxazolyl	ADRXWS	6	11.5517
12	carboxylate	4-pyrimidinyl	ADRXWS	6	11.5791
13	carboxyl	methyl	ADRXWS	6	11.1534
14	carboxyl	vinyl	ADRXWS	6	11.4127
15	carboxyl	allyl	ADRXWS	6	11.3735
16	carboxyl	methyl ketone	ADRXWS	6	11.0472
17	sulphate (so4$^-$)	2-imidazolyl	ADRXWS	6	12.9770
18	sulphate (so4$^-$)	2-pyrroryl	ADRXWS	6	13.0540
19	sulphate (so4$^-$)	3-pyrazolyl	ADRXWS	6	13.0407
20	sulphate (so4$^-$)	cyclopropane	ADRXWS	6	13.1047
21	sulphate (so4$^-$)	cyclobutadiene	ADRXWS	6	13.1721
22	phenoxy	cyclopropane	ADRXWS	6	13.5120
23	phenoxy	cyclobutane	ADRXWS	6	13.8411
24	phenoxy	cyclobutadiene	ADRXWS	6	13.5638
25	phenyl	phenyl	ADRXWS	6	13.1793
26	phenyl	imidazole	ADRXWS	6	12.3542
27	phenyl	2-imidazolyl	ADRXWS	6	12.9935
28	phenyl	phenoxy	ADRXWS	6	13.7419
29	phenyl	3-isothiazolyl	ADRXWS	6	13.3715

Table 4: Structure of designed NCEs along with predicted activity obtained by MLR equation generated by 2D QSAR

Comp ound	14X	26X	Screen result	Screen score	Predicted activity
1	ethyl	ethyl	ADRXWS	6	12.0487
2	ethyl	carboxyl	ADRXWS	6	11.4392
3	ethyl	methyl ketone	ADRXWS	6	11.9075
4	methyl	methyl	ADRXWS	6	10.4108
5	methyl	ethyl	ADRXWS	6	11.8212
6	methyl	isopropyl	ADRXWS	6	12.1216
7	methyl	vinyl	ADRXWS	6	11.6995
8	methyl	allyl	ADRXWS	6	11.8910
9	methyl	carboxyl	ADRXWS	6	11.1950
10	methyl	methyl ketone	ADRXWS	6	11.6895
11	vinyl	ethyl	ADRXWS	6	12.0482
12	vinyl	isopropyl	ADRXWS	6	12.2678
13	vinyl	vinyl	ADRXWS	6	11.8733
14	vinyl	allyl	ADRXWS	6	12.0370
15	vinyl	carboxyl	ADRXWS	6	11.3862
16	allyl	ethyl	ADRXWS	6	12.1174
17	allyl	allyl	ADRXWS	6	12.1550
18	allyl	methyl ketone	ADRXWS	6	11.9910

21	carboxyl	allyl	ADRXWS	6	11..5076
22	carboxyl	methyl ketone	ADRXWS	6	11.3314
23	carbonic	methyl	ADRXWS	6	10.8518
24	carbonic	vinyl	ADRXWS	6	11.7051

Table 5: Structure of designed NCEs along with predicted activity obtained by MLR equation generated by 2D QSAR

| Comp	14X	26X	Screen result	Screen score	Predicted activity
1	N	cyclopropane	ADRXWS	6	10.5816
2	N	cyclobutane	ADRXWS	6	10.6913
3	N	phenoxy	ADRXWS	6	10.9319
4	N	benzyl	ADRXWS	6	10.8613
5	N	bicyclohexane	ADRXWS	6	11.3721
6	S	cyclopropane	ADRXWS	6	11.7589
7	S	phenoxy	ADRXWS	6	11.9216
8	S	furan	ADRXWS	6	11.8875
9	C	cyclopropane	ADRXWS	6	12.0613
10	C	cyclobutadiene	ADRXWS	6	12.0374
11	C	pyrrole	ADRXWS	6	11.7585
12	Si	cyclopropane	ADRXWS	6	12.0156
13	Si	furan	ADRXWS	6	12.0269
14	Al	cyclobutadiene	ADRXWS	6	12.4863
15	Al	cyclopropane	ADRXWS	6	12.5103
16	Al	furan	ADRXWS	6	12.4538
17	B	benzyl	ADRXWS	6	12.4598
18	B	benzopyrrole	ADRXWS	6	12.4788
19	Ne	benzyl	ADRXWS	6	12.4600
20	Ne	benzopyrrole	ADRXWS	6	12.4790
21	methyl ketone	cyclopropane	ADRXWS	6	12.0182
22	methyl ketone	phenoxy	ADRXWS	6	11.9415
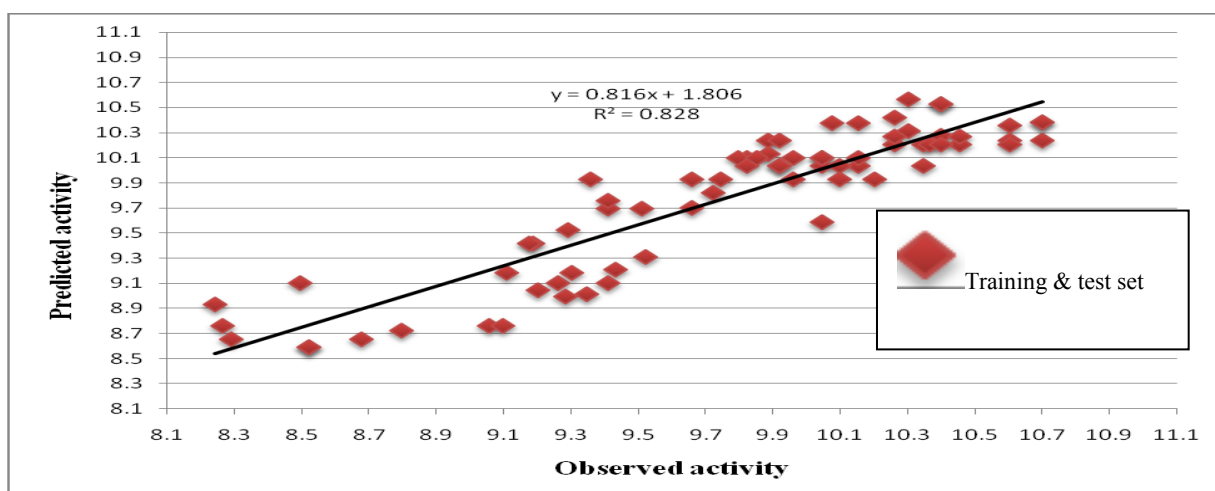
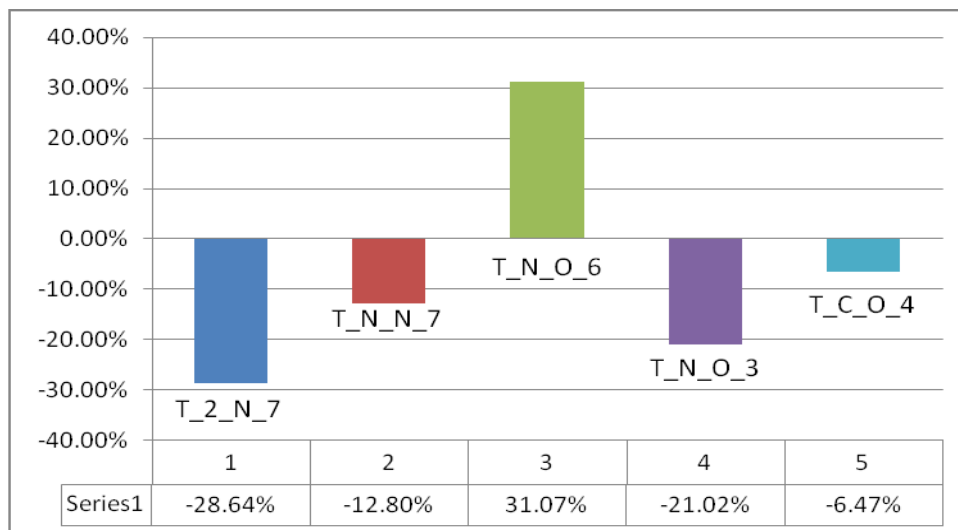**Figure 1:** Fitness plot of predicted Vs. Observed activity of 2D QSAR

Figure 2: Contribution of descriptors for biological activity developed using MLR
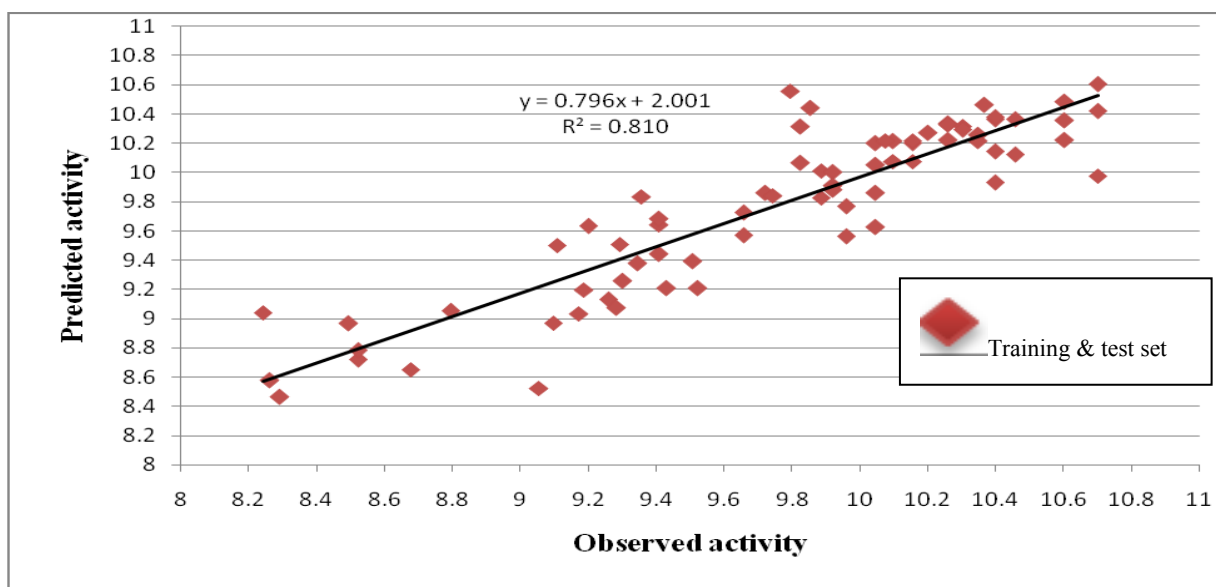

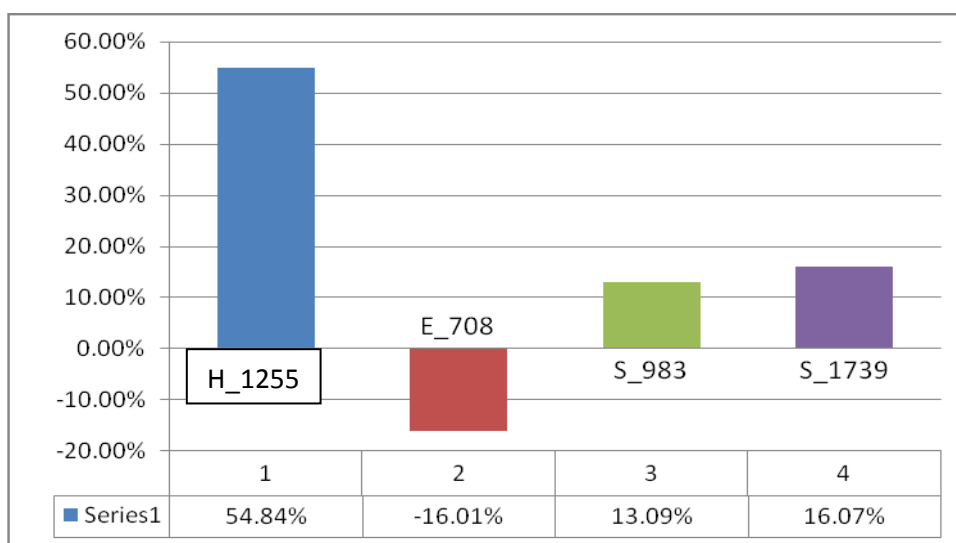**Figure 3:** Fitness plot of predicted Vs. Observed activity of 2D QSAR

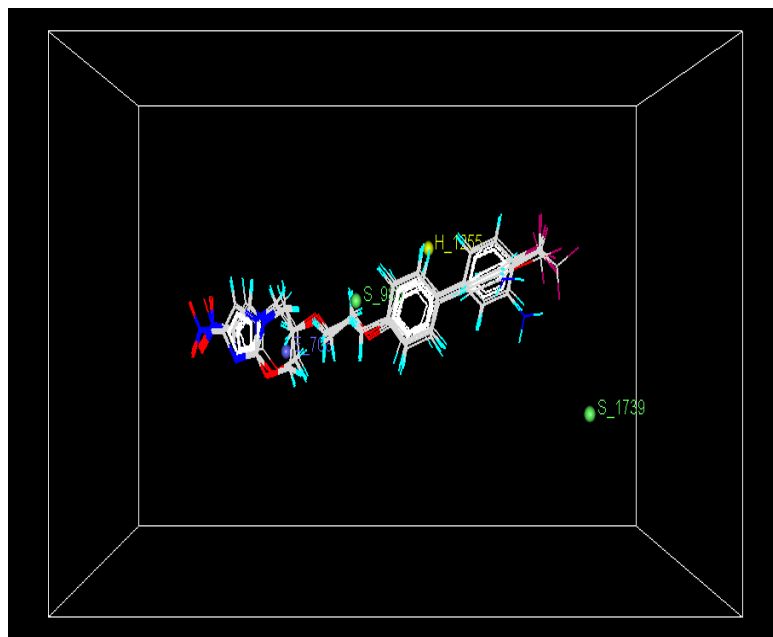**Figure 4:** Contribution plot for 3D QSAR studies of bicyclic nitroimidazole derivative

Figure 5: Stereo view of the molecular rectangular field grid around the superposed molecular units bicyclic nitroimidazole series of compounds using PCR method.

Abbreviations:
QSAR**:** Quantitative structure activity relationship
NCEs: New Chemical Entities
MLR: Multiple linear regression
PCR: Principle component regression
M.tb: Mycobacterium tuberculosis
MMFF: Merck molecular field force

REFERENCES

1. Manjunath, Ujjini; Helena IM, Boshoff and Clifton E, Barry (2009), "The mechanism of action of PA-824", ***Communicative & Integrative Biology***, 215-218.

2. Matteelli, A; Migliori, GB; Cirillo, D; Centis, R; Girard, E and Raviglion, M (2007), "Multidrug-resistant and extensively drug-resistant Mycobacterium tuberculosis: epidemiology and control (Expert Rev)", ***Anti Infect Ther***, 57-71.

3. Maroz, Andrej; Shinde, Sujata S; Franzblau, Scott G and Zhenkun, Ma *et al.* (2009), "Release of nitrite from the ant tubercular nitroimidazole drug PA-824 and analogues upon one-electron reduction in protic, non-aqueous solvent", ***Organic & Biomolecular Chemistry***, 212-223.

4. Chan, J; Tanaka, K; Carroll, D; Flynn, J and BR, Bloom (1995), "***Infect. Immune***", 736-740.

5. Stop TB Working Group, New Drugs (2008), ***www.stoptb.org/wg/newdrugs/assets/documents/2007GlobalPipeline.pdf***.

6. Stover, CK *et al.* (2000), "***Nature***", 405,962.

7. Sugawara, RI and Tohoku, J (2010), "Development of new anti-tuberculosis drug Candidates", ***Exp. Med***., 97-106.

8. Singh, R and Manjunatha *et al.* (2008), "C. E. PA-824 kills nonreplicating Mycobacterium tuberculosis by intracellular NO release", ***Science***, 1392-1395.

9. Thompson Andrew, M; Sutherland Hamish, S; Palmer Brian, D; Kmentova, Iveta and Blaser, Adrian (2011), "Synthesis and Structure Activity Relationships of Varied Ether Linker Analogues of the Antitubercular Drug (6S)-2-Nitro-6-{[4-(trifluoromethoxy)benzyl] oxy}-6,7-dihydro-5H-imidazo-[2,1-b][1,3]oxazine (PA-824)", ***J. Med. Chem***., 6563-6585.

10. Singh, Ramandeep and Manjunatha, Ujjini *et al.* (2008), "PA-824 Kills Nonreplicating Mycobacterium tuberculosis by Intracellular NO Release", ***Science***, 1392-1395.

11. (2010), "***V-Life MDS***", Version 3.5, V-Life Sciences Technologies Pvt. Ltd., Pune, India.

12. Baumann, K (2002), "An alignment-independent versatile structure descriptor for

QSAR and QSPR based on the distribution of molecular features", *J. Chem. Inf. Comput. Sci*., 42, 26-35.

13. Kirkpatrric, S; Gelatt, CD and Vecchi, MP (1983), "Optimization by simulated annealing", *Science,* 220, 671-680.

14. Golbraikh, A and Tropsha, A (2003), "QSAR modeling using chirality descriptors derived from molecular topology", *J. Chem. Inf. Comput. Sci*., 43,144-154.

Correspondence Author:
Dudhe Prashik B
Department of Pharmaceutical Chemistry,
S. T. E. S's, Sinhgad College of Pharmacy,
Email: dudhe.prashik@gmail.com

Pharmacophore (An International Research Journal)